JOURNAL OF VIROLOGY, Feb. 1975, p. 355-362

Vol. 15, No. 2
Printed in U.S.A.

Scanning Electron Microscopic Studies of Virus-Infected Cells

I. Cytopathic Effects and Maturation of Vesicular Stomatitis Virus in L2 Cells

KATHRYN V. HOLMES

Department of Microbiology, University of Texas Southwestern Medical School, Dallas, Texas 75235

Received for publication 12 September 1974

L2 cells infected with vesicular stomatitis virus under single-cycle conditions have been studied by scanning electron microscopy after preparation by the critical point drying technique. Three dimensional images of intact cells show bullet-shaped vesicular stomatitis virus virions budding singly and in radiating clusters both from the plasma membrane between cellular microvilli and from the sides of microvilli. Virus-induced cytopathic effects observed by scanning electron microscopy include intermeshing of microvilli, loss of filipodia which attach cells to the substrate, and rounding up and detachment of infected cells from the substrate.

The maturation of vesicular stomatitis virus (VSV) has been characterized in many electron microscope studies of thin sections of VSV-infected cells (4, 7, 19-21). Long strands of viral nucleocapsid appear in the cytoplasm and characteristic bullet-shaped virions develop by budding from the plasma membrane, or, in some cell types (21), into cytoplasmic vesicles. McFadden et al. (10) have estimated that as many as 10,000 virions may bud simultaneously from a single cell.

In negatively stained virus preparations the nucleocapsid strand appears to be arranged in a tightly coiled helix within the virion, and the viral envelope is covered with projections 10 nm long and 3.5 to 4.5 nm in diameter (2, 3, 7, 12, 15). Although infectious (B) virions measure 70 nm in diameter and 175 nm in length, preparations of VSV may contain noninfectious truncated VSV particles which are shorter than B virions (9).

Single-cycle growth curves of VSV in many cell types show that after a latent period of about 2 h the titer of infectious virus increases at an exponential rate until 8 to 10 h after infection (21). Synthesis of cellular RNA and protein is rapidly inhibited in infected cells (8, 11, 16-18). The characteristic cytopathic effects (CPE) of VSV infection are rounding of cells, detachment from the substrate, and lysis.

This communication describes a scanning electron microscope (SEM) study of VSV maturation and CPE. The unique stereoscopic images of the surfaces of infected cells have revealed that virions bud both singly and in radiating clusters, virions develop both from the plasma membrane over the cell body and from microvilli, and that major changes in cell surface organelles such as microvilli, filipodia, and ruffled membranes result from virus infection.

MATERIALS AND METHODS

Cell cultures. The L2 variant of the L929 line of mouse fibroblasts, obtained from L. Sturman, New York State Department of Public Health, Albany, N.Y., was grown in monolayers on glass coverslips in Dulbecco's modification of Eagle minimal essential medium (5) with 10% heat-inactivated fetal calf serum with 100 U of penicillin, 100 μg of streptomycin, and 0.25 μg of fungizone per ml in 5% CO_2 at 37 C.

Virus strain. The Indiana serotype of VSV was obtained from E. Sulkin's laboratory, Southwestern Medical School, Dallas, Tex., where it had been passaged in L2 cells.

Virus inoculation. Confluent monolayers of L2 cells on glass coverslips in 60-mm plastic petri dishes were inoculated with 0.5 ml of VSV at a multiplicity of infection of about 10 PFU per cell. Control monolayers were sham inoculated with 0.5 ml of medium. After absorption for 1 h at 37 C, the inoculum was removed and the cell monolayers were overlaid with growth medium and incubated in 5% CO_2 at 37 C. At intervals, monolayers of control and infected cells were fixed and prepared for SEM.

Preparation of specimens for SEM. Cells were fixed in situ on glass coverslips with glutaraldehyde (14). Glutaraldehyde was added to the medium in the petri dish to a final concentration of 1%, and the cells were fixed for 1 h at 37 C. In all subsequent steps, care was taken to keep the surface of the coverslip under fluid to prevent distortion of cells. The medium containing glutaraldehyde was replaced with 1% glutaraldehyde in phosphate-buffered saline (6) and the cells were held at 4 C for 1 to 4 days. Fixed monolayers were gradually dehydrated after the method of Ander-

son (1) in serial 15-min changes of 30, 50, 70, 95, and 100% ethanol followed by two 15-min treatments with amyl acetate. In a Polaron critical point drying apparatus, the amyl acetate was replaced by liquid CO_2. The CO_2 was brought to the critical point and the carbon dioxide gas was released. The specimens were then coated with a layer approximately 10 nm thick of gold or gold and palladium in a Mikros carbon evaporator with a rotary coater attachment and observed with a JEOL JSM-35U or an ETEC model 1000 scanning electron microscope at 20 to 25 kV accelerating voltage. Stereoscopic photograph pairs were taken with 6° difference in specimen tilt and observed with a fixed focus stereoscopic viewer (Fullam, Inc., Schenectady, N.Y.).

RESULTS

Morphology of normal L2 cells. In sham-inoculated control monolayers, L2 cells appeared as spindle-shaped or polygonal cells (Fig. 1). Several different types of surface projections could be identified (13). The cells were attached to the glass substrate and to each other by long, rigid filipods. Ruffled membranes were observed at the edges of most cells and the cell surface was studded with curving, cylindrical, unbranched microvilli with rounded tips. The microvilli were of varying lengths but most had a diameter of about 100 nm. On the surface of some cells were large rounded projections which have been called blebs. Between these projections, the cell surface was smooth. In subconfluent monolayers of uninfected cells, rounded dividing cells could be observed attached to the coverslip by numerous filipods.

Budding of VSV virions. About 4 h after infection with VSV, numerous short, rigid, bullet-shaped projections could be seen budding perpendicular to the cell surface between the microvilli. The diameter of the short projections was usually slightly less than that of the microvilli. These short projections were believed to be VSV virions budding from the plasma membrane, since at this time after infection both transmission electron microscopy (TEM) and infectivity assays indicated that extensive virus budding was occurring. Also, comparable numbers of such short projections were not observed in uninfected control cells. In single photographs the presumptive virions appeared to be of varying length because of the different angles at which they projected from the cell. When stereoscopic images were observed, however, the virions appeared to be of uniform length, suggesting that there were few truncated particles in this preparation.

Figure 2 shows many VSV virions budding

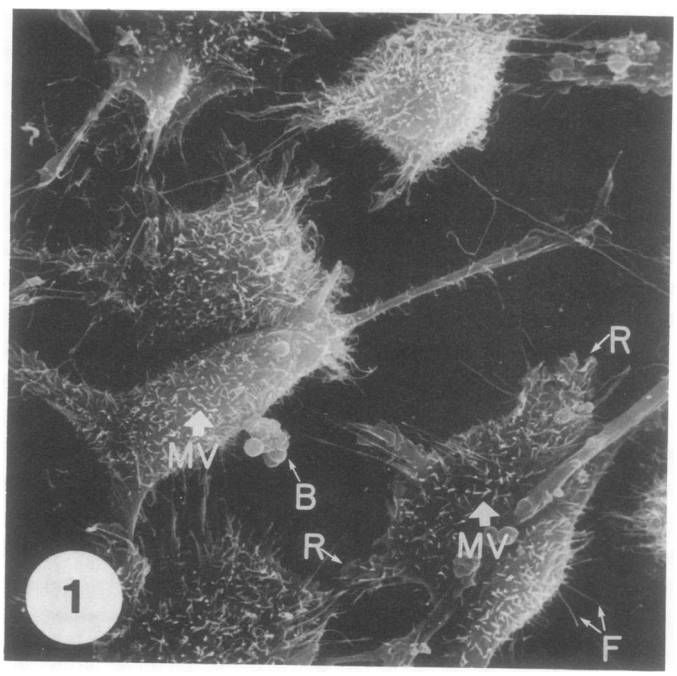

FIG. 1. *Uninfected L2 cell monolayer fixed with glutaraldehyde, prepared by the critical point drying technique, coated with gold and palladium, and viewed by SEM. The uninfected cells are elongated or polygonal with a smooth surface studded with numerous curving, cylindrical, unbranched cellular microvilli (MV). The cells are attached to the substrate by elongated, rigid filipodia (F). Ruffled membranes (R) are present at the cell borders. Large rounded blebs (B) are observed on the membranes of some cells.* ×2,000.

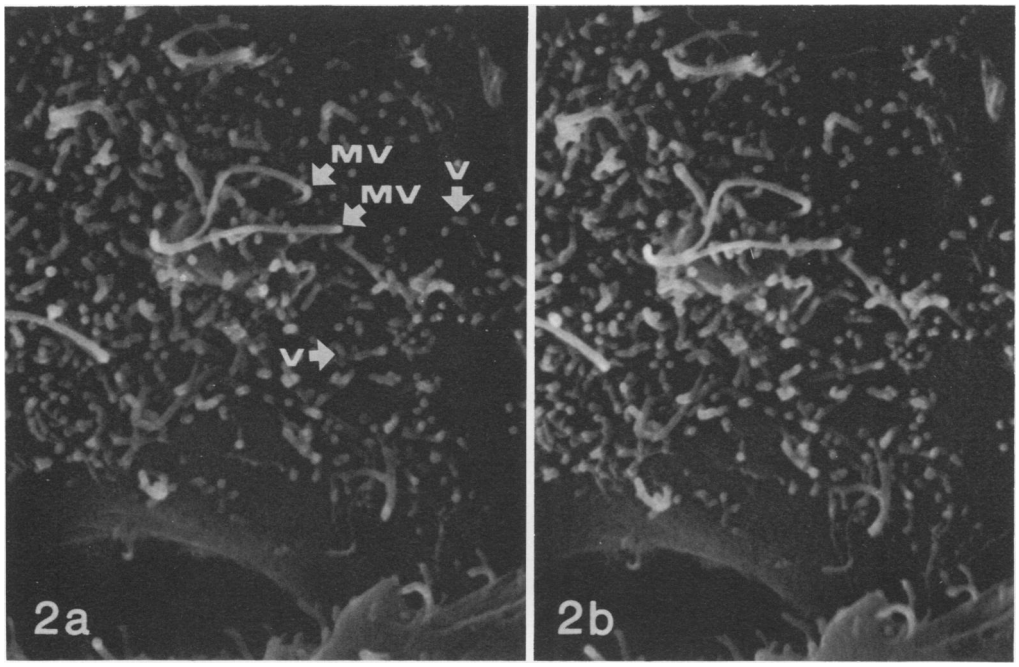

FIG. 2. *VSV virions budding from the plasma membrane of an infected L2 cell 8 h after virus inoculation. The virions (V) appear as numerous short, rigid rods with rounded ends budding perpendicular to the smooth, flat portion of the plasma membrane between the longer curving cellular microvilli (MV). The horizontal arrow labeled V indicates a virion budding from a microvillus. Fig. 2a and b are stereoscopic images photographed with a difference of 6° in specimen tilt. To obtain a three-dimensional image they should be observed with a stereoscopic viewer. ×13,000.*

from the cell surface between microvilli as well as from the sides of microvilli at 8 h after virus inoculation. Virions budding from the cellular microvilli gave them a branching appearance not seen in microvilli on control cells. VSV virions budded perpendicular to the plasma membrane and were readily distinguished from absorbed virions which were observed in preparations held at 4 C to be attached to the cell membrane by the sides of the virion rather than by the end. VSV virions frequently were observed budding in clusters radiating from a single point on the surface of an infected cell (Fig. 3). Budding clusters of two to five or more virions have been observed by SEM.

As the cells began to round up, the number of VSV virions seen budding from the plasma membrane increased. The stereoscopic image of the rounded fibroblastic cell in Fig. 4 makes it possible to see that extensive budding of virions from cellular microvilli caused them to appear branched. As the virions budded, they often appeared to adsorb to other cellular microvilli from which viruses could be budding, forming an intricate network of adsorbed viruses and cellular processes around the cell. In Fig. 5 at a higher magnification, the intimate association of budding virions with microvilli can be seen without the stereoscopic image. Unfortunately, it was not possible to resolve viral surface projections on the budding virions because the limit of resolution of the microscopes used in this study was 10 nm. Unequivocal identification of any individual surface projection as a virus rather than an unusually slender and short microvillus is therefore not possible by this technique. Virus-specific antigens might be visualized on infected cells incubated with hybrid antibody directed against the antigens and against a visible marker such as tobacco mosaic virus. This technique has been successfully used to localize antigens on the surface of lymphocytes observed by SEM (M. L. Lipscomb, K. V. Holmes, E. S. Vitetta, U. Hämmerling, J. W. Uhr, submitted for publication).

The surface of infected cells by 17 h after virus inoculation was almost completely covered with budding VSV virions (Fig. 6 and 7). It seems probable that these virions were arrested in the process of budding because little infectious virus was released from infected cell monolayers at this time. Projecting from the cells were a small number of markedly elongated microvilli from which clusters of VSV virions were bud-

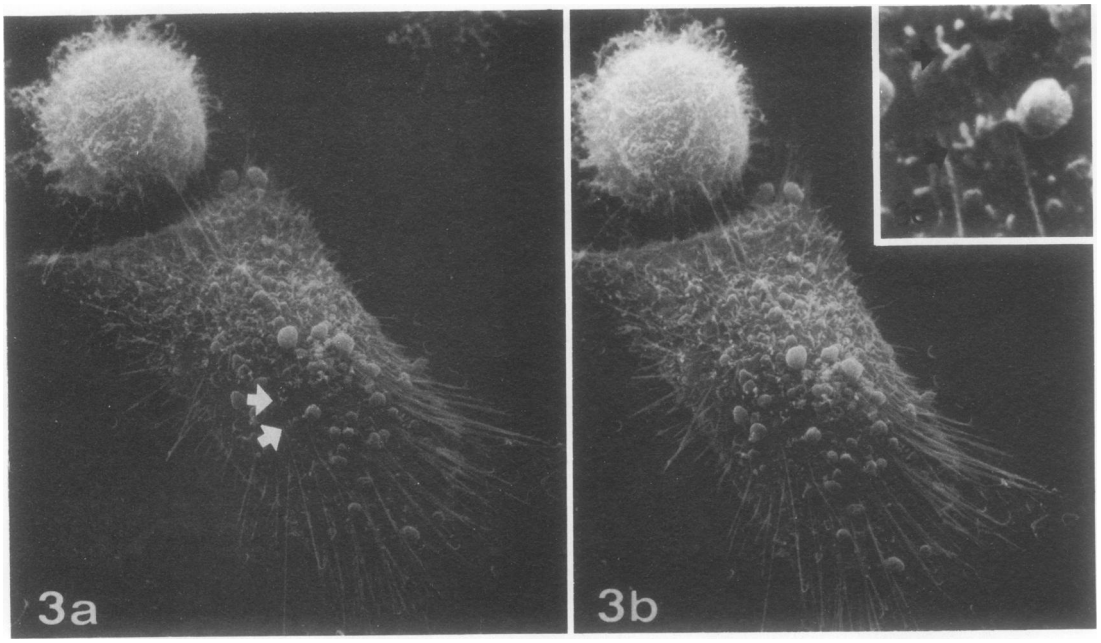

FIG. 3. *Stereoscopic SEM images of two VSV-infected L2 cells showing virus-induced CPE and budding virions. As a result of VSV infection, the cell at the upper left has rounded up and lost most of the filipodia which attached it to the substrate. The central cell, which is beginning to round up as a result of VSV infection, is still attached to the substrate by numerous filipodia. The virions shown at the tips of the arrows and in the inset (c) are budding in clusters which radiate from a single point on the cell surface. Such multiple virus buds are frequently observed in VSV-infected cells. The multiple buds are usually of equal length when seen in stereo images. ×2,500, inset ×8,400.*

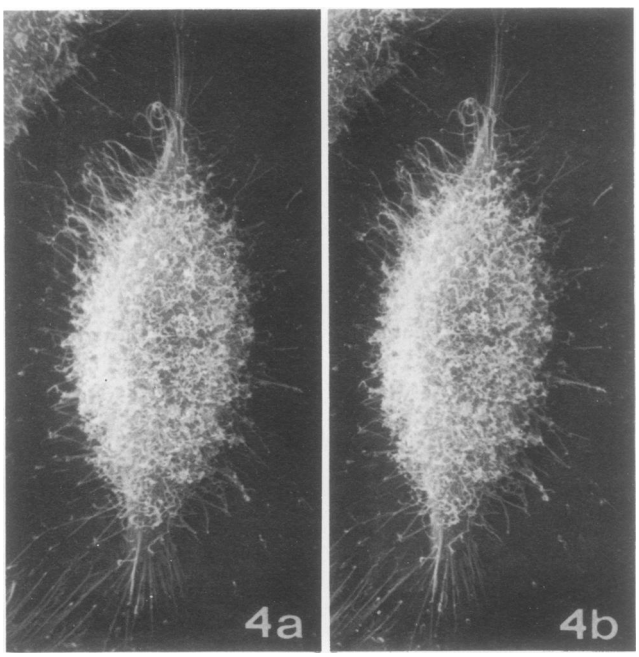

FIG. 4. *Stereoscopic SEM images of a fibroblastic cell 17 h after VSV inoculation. Numerous virions budding from the cellular microvilli give these a brushlike appearance not seen in uninfected control cells. The budding viruses are often absorbed to the surface of the cell or to other microvilli, forming an intermeshing network of viruses and cellular processes around the infected cell. Compare with control cells in Fig. 1. ×2,000.*

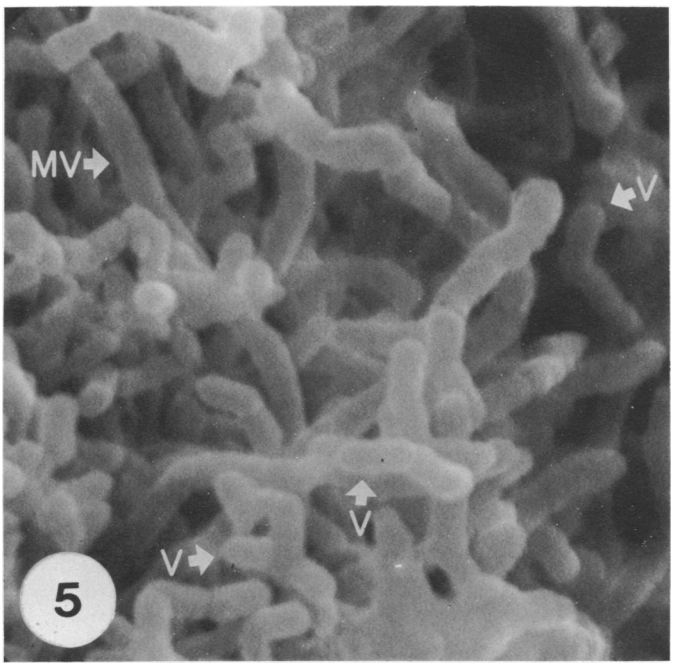

FIG. 5. *High magnification of a VSV-infected cell like that shown in Fig. 4. The numerous projections from the cell surface include both microvilli (MV) and VSV virions (V). The microvilli are longer and are slightly larger in diameter than the virions. Virions budding from the sides of microvilli make them appear to be branching. Fine details of the virion surface such as virus spikes are not resolved in this preparation.* ×45,000.

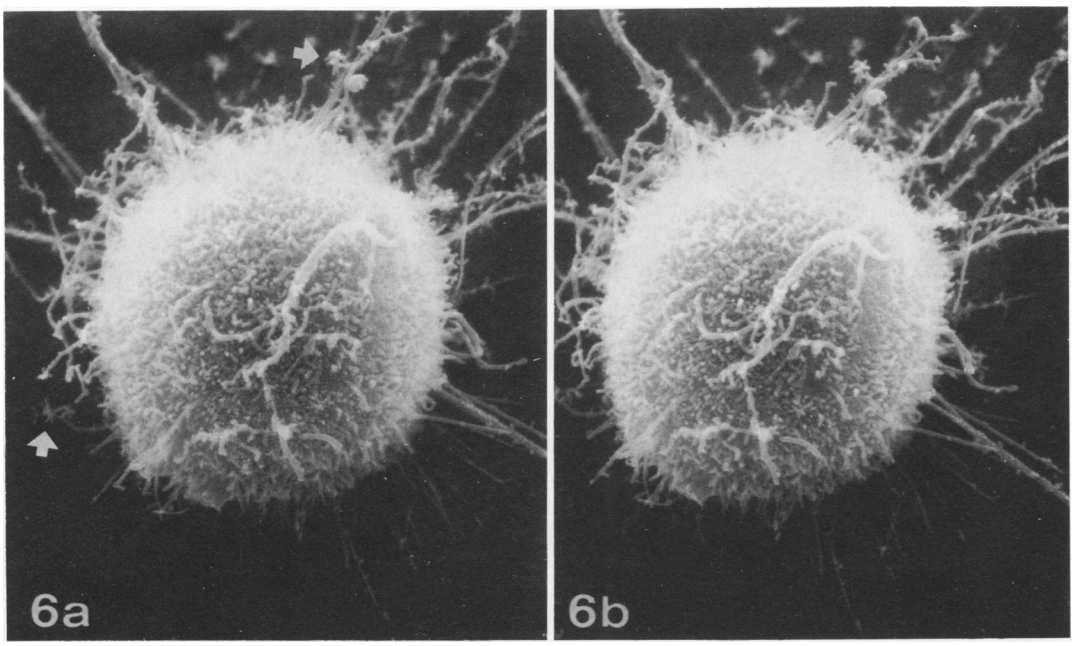

FIG. 6. *Stereoscopic SEM images of VSV-infected L2 cell 17 h after virus inoculation. The infected cell has rounded up and is attached to the substrate by a few filipods. Most of the cell surface is covered with budding virions (See Fig. 7), which have replaced most of the microvilli. The remaining microvilli are elongated and frequently appear brushlike due to the budding of virions from the sides of the microvilli. Arrows indicate areas where radiating clusters of virions are budding at a great distance from the cell body.* ×5,000.

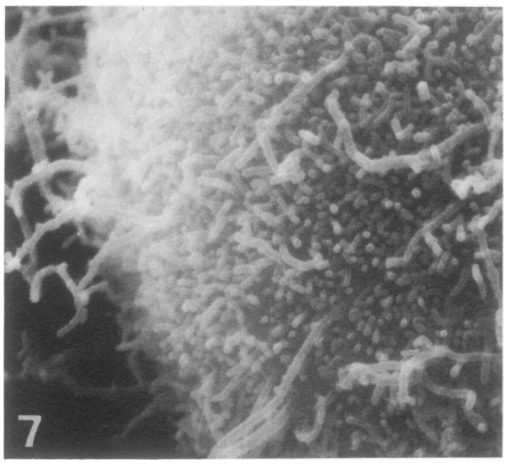

FIG. 7. *Higher magnification of the lower left portion of the cell shown in Fig. 6. The budding VSV virions can be clearly seen both on the cell surface and budding from microvilli.* ×*10,000.*

ding. Some of these microvilli were more than 5 μm long. In TEM studies viruses budding from microvilli at such great distances from the cell body might be incorrectly interpreted as virions that had been released into the medium. SEM, by permitting observation of the entire cell, shows that these budding virions are still attached to the cell.

Development of VSV-induced CPE. As more and more budding virions appeared on the surface of infected cells, major changes in cell surface organelles occurred. By 8 h after virus inoculation, many cells were beginning to show CPE. These cells (like that in Fig. 4) had no ruffled membranes and showed numerous microvilli with budding viruses.

The nature of the microvilli changed extensively as infection progressed. In addition to the branching and sometimes brushlike appearance of microvilli due to the presence of budding virions (Fig. 4 and 6), infected cells often showed very elongated microvilli. These may have been remnants of filipodia which had detached from the substrate. Because there is no identifiable surface substructure by which virions can be distinguished from microvilli, SEM alone cannot prove that these long structures are of cellular rather than viral origin. In thin sections of VSV-infected cells, unusually long budding virions with nucleocapsid extending the full length of the virion have occasionally been observed (10). However, since these represent an unusual occurrence and the present study reports elongated projections from almost every cell late in infection, it appears more likely that the elongated structures were indeed cellular microvilli.

Virus-induced changes in cell shape have been visualized in three-dimensional images with the SEM. Some infected cells had begun to round up by 8 h after VSV inoculation. As the previously flattened cells began to round up, numerous filipods could be seen attaching the cells to the substrate (Fig. 3). However, as the CPE progressed and the cells assumed a spherical shape, the number of filipods anchoring the cells was markedly reduced (Fig. 3 and 6). At the final stage of infection the few remaining filipods detached and the infected cells, studded with virus particles, floated free in the medium.

DISCUSSION

Ultrastructural studies of virus-infected cell monolayers by SEM offers several unique advantages over conventional techniques of TEM. (i) The SEM permits the study of large numbers of whole cells in situ and therefore reduces the sampling errors inherent in studies done on thin sections of infected cells. (ii) The development of virus-induced CPE can be studied in intact cells with stereoscopic photographs. Interactions of infected cells with each other and with the substrate can readily be observed. Virus-induced alterations in the normal cell surface and its organelles such as microvilli, filipodia, ruffled membranes, etc., can be detected best by SEM. (iii) The maturation of virions can be observed in three-dimensional images and the distribution of virus budding at different sites on the cell surface can readily be mapped.

These advantages are, however, dependent upon the technique used to prepare infected cells for SEM. When infected cells were fixed in glutaraldehyde, dehydrated and air-dried from a variety of solvents, gross distortion of the cells resulted. Virions were obliterated or appeared collapsed onto the surface of the cell (K. V. Holmes, unpublished data). Gluteraldehyde fixation (14) and subsequent dehydration by the critical point drying method (1, 13) yielded cells in which normal three-dimensional structure was retained and delicate surface organelles such as microvilli and ruffled membranes were well preserved (Fig. 1). With these techniques it was possible to see three-dimensional images of whole virus-infected cells showing budding of individual virions (Fig. 2 to 4, 6).

The SEM studies reported in this paper demonstrate that major structural changes in the plasma membrane of L2 cells occurred as a result of VSV infection. After infection, virus

buds developed and progressively covered more and more of the cell surface. In preparations such as these, SEM shows only those virus buds which were still attached to the cell. Virions that had matured and had been released would have been washed away during preparation for SEM. Late in infection, when the cellular metabolic activity is known to be markedly reduced (8, 11, 16–18), and the yield of released virus is very small (21), the surfaces of all the cells were covered with budding virions. It is possible that maturation of these virions was arrested because they could not be released from the infected cell. The process of viral budding and release may be much faster during the period of exponential rise of released virus than in the rounded up cells at the end stage of VSV-induced CPE. In addition, the observation that 17 h after infection most of the budding virions seen in three-dimensional images were about the same length suggests that the development of the bullet-shaped virion may be faster than its release. Similarly, the presence of clusters of budding virions on the surface of infected cells could represent aberrant developmental forms that could not be released normally from cells and therefore stayed at the cell membrane for a longer time. Although such multiple buds of VSV have occasionally been observed by TEM (20), the frequency of these aberrant forms can be determined best by SEM.

Previous reports of CPE induced by VSV indicated that infected cells rounded up, detached from the substrate, and floated away into the medium. This study shows that as infection progressed, there was a great reduction in the number of cellular filipodia, the delicate organelles of the plasma membrane by which cells attach to the substrate or to each other. Whether this resulted from usurpation of cell membrane by virus buds or an internal metabolic alteration caused by VSV infection must be determined. SEM studies of persistent virus infections in vitro in which virus production can proceed at high levels for long periods would be useful to show the interactions between virus budding and organelles of the plasma membrane that are compatible with long life of the infected cell. Clearly, nutrients needed for both cell and virus-specific syntheses of nucleic acids, lipids, and proteins must be able to enter via the plasma membrane if the infected cell is to remain viable. What proportion of the normal cell membrane is needed to preserve these functions remains to be determined.

ACKNOWLEDGMENTS

I thank Patricia Wiesner for expert technical assistance and A. Kabaya for help and advice. Scanning electron microscopes were generously made available by the Mostek Corp., Carrollton, Tex., JEOL Inc., Medford, Mass., and the Department of Pathology at Southwestern Medical School.

These studies were supported by Public Health Service grant CA14517 from the National Cancer Institute and grant PO1-AI-11851 from the National Institute of Allergy and Infectious Diseases.

LITERATURE CITED

1. Anderson, T. F. 1951. Techniques for the preservation of three dimensional structure in preparing specimens for the electron microscope. Trans. N.Y. Acad. Sci. Ser. 2 **13**:130–134.
2. Bergold, G. H., and K. Munz. 1967. Ultrastructure of Cocal, Indiana and New Jersey serotypes of vesicular stomatitis virus. J. Ultrastruct. Res. **17**:233–244.
3. Cartwright, B., C. J. Smale, F. Brown, and R. Hull. 1972. Model for vesicular stomatitis virus. J. Virol. **10**:256–260.
4. David-West, T. S., and N. A. Labzoffsky. 1968. Electron microscopic studies on the development of vesicular stomatitis virus. Arch. Gesamte Virusforsch. **23**:105–125.
5. Dulbecco, R., and G. Freeman. 1959. Plaque production by the polyoma virus. Virology **8**:396–397.
6. Dulbecco, R., and M. Vogt. 1954. Plaque formation and isolation of pure lines with poliomyelitis viruses. J. Exp. Med. **99**:167–182.
7. Howatson, A. F., and G. F. Whitmore. 1962. The development and structure of vesicular stomatitis virus. Virology **16**:466–478.
8. Huang, A. S., D. Baltimore, and M. Stampfer. 1970. Ribonucleic acid synthesis of vesicular stomatitis virus. III. Multiple complementary messenger RNA molecules. Virology **42**:946–957.
9. Huang, A. S., J. W. Greenwalt, and R. R. Wagner. 1966. Defective T particles of vesicular stomatitis virus. I. Preparation, morphology and some biologic properties. Virology **30**:161–172.
10. McFadden, G. K., R. L. Truitt, and I. L. Schechmeister. 1973. Ultrastructural examination of phytohemagglutinin stimulated lymphocytes infected with vesicular stomatitis virus. Arch. Gesamte Virusforsch. **41**:229–237.
11. Mudd, J. A., and D. F. Summers. 1970. Protein synthesis in vesicular stomatitis virus-infected HeLa cells. Virology **42**:328–340.
12. Nakai, T., and A. F. Howatson. 1968. The fine structure of vesicular stomatitis virus. Virology **35**:268–281.
13. Porter, K. R., D. Kelley, and P. M. Andrews. 1972. The preparation of cultured cells and soft tissues for scanning electron microscopy, p. 1–19. Proc. Fifth Annu. Stereoscan Colloq. Kent Cambridge Scientific Co., Morton Grove, Ill.
14. Sabatini, D. D., K. Bensch, and R. J. Barrnett. 1963. Cytochemistry and electron microscopy. The preservation of cellular ultrastructure and enzymatic activity by aldehyde fixation. J. Cell Biol. **17**:19–58.
15. Simpson, R. W., and R. E. Hauser. 1966. Structural components of vesicular stomatitis virus. Virology **29**:654–667.
16. Wertz, G. W., and J. S. Youngner. 1970. Interferon production and inhibition of host synthesis in cells infected with vesicular stomatitis virus. J. Virol. **6**:476–484.
17. Wertz, G. W., and J. S. Youngner. 1972. Inhibition of protein synthesis in L cells infected with vesicular

stomatitis virus. J. Virol. **9**:85–89.
18. Yamazaki, S., and R. R. Wagner. 1970. Action of interferon: kinetics and differential effects on viral functions. J. Virol. **6**:421–429.
19. Yang, Y. J., D. B. Stoltz, and L. Prevec. 1969. Growth of vesicular stomatitis virus in a continuous culture line of *Antheraea eucalypti* moth cells. J. Gen. Virol. **5**:473–483.
20. Zajac, B., and K. Hummeler. 1970. Morphogenesis of the nucleoprotein of vesicular stomatitis virus. J. Virol. **6**:243–252.
21. Zee, Y. C., A. J. Hackett, and L. Talens. 1970. Vesicular stomatitis virus maturation sites in six different host cells. J. Gen. Virol. **7**:95–102.